FEM-DBEM coupled procedure for assessment of cracks in lateral supports of the magnet system of Wendelstein 7-X

R. Citarella, M. Lepore
Dept. of Industrial Engineering, Univ. of Salerno, Italy
rcitarella@unisa.it

Joris Fellinger, Victor Bykov, Felix Schauer
Max Planck Institute for Plasma Physics, EURATOM Association, Wendelsteinstr. 1, 17491 Greifswald, Germany

ABSTRACT. The superconducting coils of the magnet system of Wendelstein 7-X (W7-X) are bolted onto a central support ring and interconnected with five so-called lateral support elements (LSEs) per half module. After welding of the LSE hollow boxes to the coil cases, cracks were found in the vicinity of the welds that could potentially limit the allowed number *N* of electromagnetic (EM) load cycles of the machine. In response to the appearance of first cracks during assembly, the stress intensity factors (SIFs) were calculated and corresponding crack growth rates of theoretical semi-circular cracks of measured sizes in potentially critical position and orientation were predicted using Paris' law, whose parameters were calibrated in fatigue tests at cryogenic temperature. The Miner's rule was adopted to allow for different load combinations. The predefined semi-circular initial crack shape and crack growth limit, were set in such a way to avoid multiple crack coalescence even if such restrictions could have a significant effect on *N*. These results have been published in a first paper, whereas, in the current paper, this work has been extended with analyses of propagation of cracks with different shapes and affected by nearby cracks. For this purpose, the Dual Boundary Element Method (DBEM) was applied in a coupled FEM-DBEM approach: the crack path is assessed with the Minimum Strain Energy density criterion and the SIFs are calculated by the J-integral approach. The Finite element method (FEM) was adopted to model the overall component whereas the DBEM was adopted for the submodel analysis in the volume surrounding the cracked area. With this approach, the effects of the crack shape and the presence of nearby cracks on the allowed number of EM load cycles of the machine were demonstrated.

SOMMARIO. I nuclei superconduttori del sistema magnetico di Wendelstein 7-X (W7-X) sono collegati tramite bulloni su un anello di supporto centrale e connessi tra loro tramite cinque cosiddetti elementi di supporto laterale (LSE) per ogni metà modulo. A valle della saldatura tra gli elementi scatolari LSE e i nuclei superconduttori fu evidenziata la presenza di cricche in prossimità delle saldature che potenzialmente potevano limitare il numero consentito N di cicli elettromagnetici da applicare alla macchina. In conseguenza dell'apparizione delle prime cricche durante la fase di assemblaggio, si è proceduto al calcolo degli Stress Intensity Factors (SIFs) e, tramite la formula di Paris (calibrata con test di fatica a temperatura criogenica), al calcolo delle corrispondenti velocità di accrescimento, per cricche di forma iniziale semicircolare e dimensioni come da evidenza sperimentale, collocate in posizione e con orientazione potenzialmente critiche. La legge di Miner, di accumulo del danno lineare, è stata adottata al fine di considerare differenti combinazioni di carico. In un precedente lavoro [1] si ipotizzava una forma semicircolare per una singola cricca e dei limiti di accrescimento tali da non incorrere in situazioni di potenziale coalescenza tra cricche diverse, anche se tali ipotesi restrittive determinavano una notevole diminuzione del numero di cicli ammissibile. In questo lavoro si

cerca di rilassare le limitazioni imposte dalle precedenti assunzioni, con la considerazione di cricche multiple interagenti e di forma iniziale anche semiellittica. A tale scopo si fa riferimento ad una procedura accoppiata FEM-DBEM (Dual Boundary Element Method) nella quale il percorso di propagazione è definito sulla base del criterio della Minima Densità di Energia Deformazionale mentre i SIF sono calcolati a partire dal J-integral. In ambiente FEM si procede alla modellazione del componente globale mentre l'analisi di un sottomodello (estratto dal precedente) costituito dal volume circostante la cricca è realizzata in ambiente DBEM. Con tale approccio è possibile valutare gli effetti della geometria della cricca iniziale e della presenza di cricche adiacenti sul numero di cicli di carico ammissibili sulla macchina.

KEYWORDS. FEM-DBEM; Superconductive coils; Crack propagation; Elettro-magnetic cycles.

INTRODUCTION

The fivefold symmetric modular stellarator Wendelstein 7-X (W7-X) is currently under construction in Greifswald, Germany [1]. Each of the five modules are build up of two flip symmetric half modules (ten in total) which consist of 5 non-planar (NP) and 2 planar superconducting coils each to be operated at 4K, see Fig. 1. The NP coil cases are made of cast stainless steel (SS) EN 1.3960. They are bolted onto a SS central support ring and welded together at the outboard side of the torus via the LSE's consisting of 100 – 150 mm long hollow tubes of 30 – 35 mm thick forged SS EN 1.4429 (see Fig. 1). After welding the LSEs (weld depth 15-30 mm), many surface cracks substantially larger than 8 mm (typical acceptance limit of EN 23277) were found with dye penetration tests at the accessible surfaces, particularly at the coil side of the weld within the cast steel, oriented parallel to the weld seam.

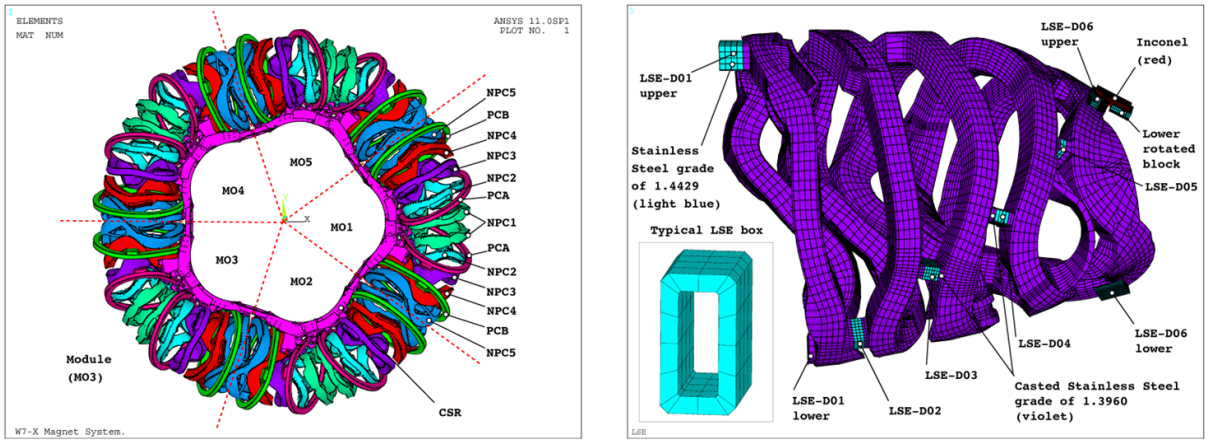

Figure 1: Fivefold symmetric FE model of the magnet system of Wendelstein 7-X (left) and detail of a half module where the LSE's are shown.

In a first paper [2], the averaged SIF along the crack front of these cracks were predicted using an analytical method and finite element method (FEM) models which were benchmarked against each other and against a single run with a boundary element method (BEM) model. Based on Paris' law parameters derived from 10 fatigue crack growth rate tests (FCGR) carried out at cryogenic temperature at Karlsruhe Institute of Technology (KIT), the predicted SIF could be related to cyclic crack growth. Assuming proportionality between the SIF and square root of the crack size ($\Delta K \propto \sqrt{a}$) and an arbitrary maximum crack size, it was possible to derive the number of load cycles until failure from the SIF of the initial crack. The maximum radial crack size increase was limited to 10 mm to avoid coalescence of the observed crack with adjacent cracks and to ensure that the crack remains small compared to the cross section, i.e. to ensure the proportionality rule $\Delta K \propto \sqrt{a}$. Clearly, the maximum crack size limit has an important influence on the predicted number of cycles.

In the current paper, the assessment is extended for the most critical crack using the Dual Boundary Element Method (DBEM) [3-5]. This most critical crack was located in LSE-D05 in the cast steel, see Fig. 1. In the DBEM method, the stress state and SIFs along the crack front are updated at each step of crack advance. As a consequence, deviation from the proportionality rule is automatically simulated. Moreover, an adjacent crack was included in the model which allows for the simulation of crack coalescence. So, no maximum crack size needs to be defined and crack growth can be continued until the critical SIF is reached, i.e. the SIF where unstable crack growth starts. In addition, the method calculates the crack growth rate along the crack front rather than assuming a pure radial growth. So, it enables the prediction of crack growth of non-circular cracks. The depth of the crack is fundamentally unknown but from repair experience it was found that the crack depth was typically smaller than half the crack length. To verify the influence of the assumed crack shape, a semi-elliptical crack has been compared with the original semi-circular crack.
In the next section, the DBEM and FEM models are presented and the results of the DBEM model in comparison with the results that were previously obtained with the FEM model are discussed. Also, the effect of adjacent crack and elliptical crack shape is evaluated. Finally in section four, the conclusions are given.

MODELS AND RESULTS

Since the mechanical behaviour of the magnet system is of crucial importance for the operation of W7-X, two independent global FEM models of the magnet system have been developed (one in Ansys and one in Abaqus) which are successfully benchmarked against each other. The original FEM analysis around the most critical crack has been made using a local model around the crack in Abaqus loaded with imposed displacements from the Abaqus global model. The new DBEM model however, is loaded with the imposed displacements from the Ansys global model because no interface between the BEM software and Abaqus was at disposal. But the displacements and generalised sectional forces and moments typically deviate less than 10% between both global models.

FEM model

In the preparation of the FEM submodel it was found that it suffices to include in the submodel only the LSE without the adjacent coils. So only LSE D05 was modelled with the semi-circular crack of 14 mm diameter at the outside of the cast steel, see Fig. 2. The crack is modelled as a seam in the mesh with elements following the contour of the crack. At the same time, it was found that the results are sensitive to the modelling of the weld. Notably, the weld does not penetrate through the entire thickness of the forged steel tube, so part of the cross section remains un-welded, see right picture of Fig. 2. If the un-welded area is at the outside of the cross section, it shields the crack from stresses perpendicular to the crack. Vice versa, the perpendicular stresses around the crack are increased when the un-welded area is at the inside of the cross section. For the critical crack under consideration, the stresses perpendicular to the crack are increased.

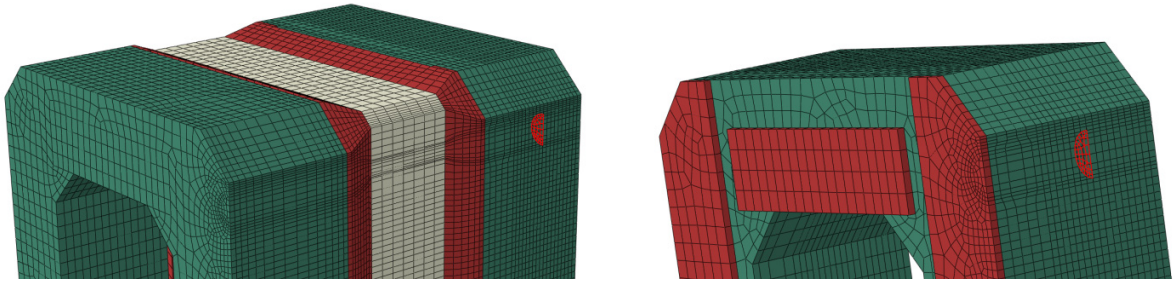

Figure 2: Zoom of the FEM submodel of the critical crack of 14 mm diameter in LSE D05 (left) and cut through the weld (right) to show the penetration depth of the weld and the cold contact zones.

Since the mesh is adapted to the crack shape and size, the model does not allow for simulation of crack growth. Along the crack tip, the J-integral is requested as output. The averaged value of the J-integral is used to calculate an effective SIF K as

$$K = \sqrt{J \frac{E}{1-\nu^2}} \tag{1}$$

With Young's modulus E = 158 GPa and Poison's ratio ν = 0.3.

From the simulations it was found that K depends on the EM load configuration. At the initial crack size radius $a_i = 7$ mm, K_i reaches a maximum of 46 MPa√m. Allowing a crack growth up to a radius of 17 mm and assuming the proportionality rule $\Delta K \propto \sqrt{a}$, one obtains at the ultimate crack size $K_u = \sqrt{\frac{a_u}{a_i}} K_i$, which reaches 72 MPa√m. This value is still below the critical value K_{Ic} =106 72 MPa√m.

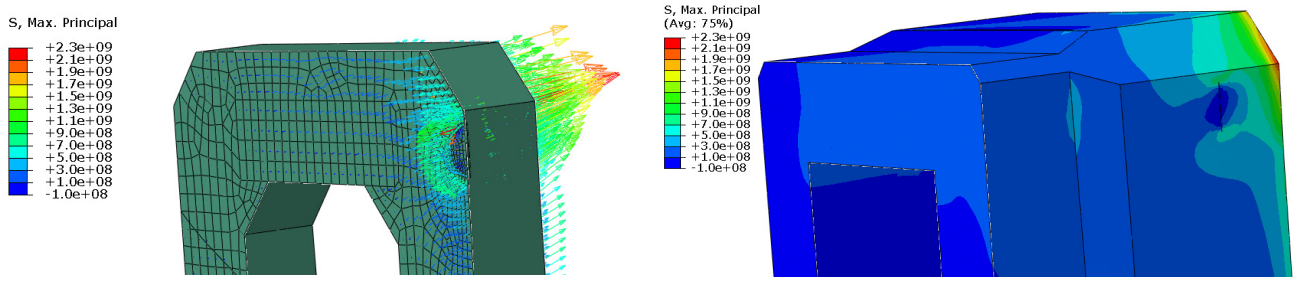

Figure 3: Maximum principal stress under EM load for the cast steel around the crack.

DBEM submodel description and result analysis

The DBEM submodelling is aimed at analyzing the propagation of cracks with elliptical or semicircular shapes and, eventually, affected by nearby cracks. For this purpose, the Dual Boundary Element Method (DBEM) was applied in a coupled FEM-DBEM approach with the crack path assessed by the Minimum Strain Energy density criterion and the Stress Intensity Factors (SIFs) calculated by the J-integral approach [3-5]. The Finite Element Method (FEM) was adopted to model the overall component whereas the DBEM was adopted for the submodel analysis in the volume surrounding the cracked area. The boundary conditions applied on the DBEM local model surrounding the crack are the displacements calculated from the magnet system global model (Fig. 1), loaded with a magnetic field equal to 3 T (Tesla). In particular a DBEM thermal-stress analysis was needed in order to also allow for the coil cooling from an ambient temperature equal to 293 K to the superconductive temperature equal to 4 K, and subsequent electromagnetic loading from 0 to 3 Tesla. In Fig. 4 the DBEM submodel is shown, as obtained by a Boolean operation of subtraction of a spherical domain from the Ansys overall model; the sphere center coordinates are x= 5.56659 m, , y=2.95385 m, z =0.476757 m and the radius is equal to 0.15 m (with such value the submodel is judged sufficiently bigger than the cracked area); in the same figure the submodel splitting in 5 zones, with different material properties (Tab. 1), is highlighted.

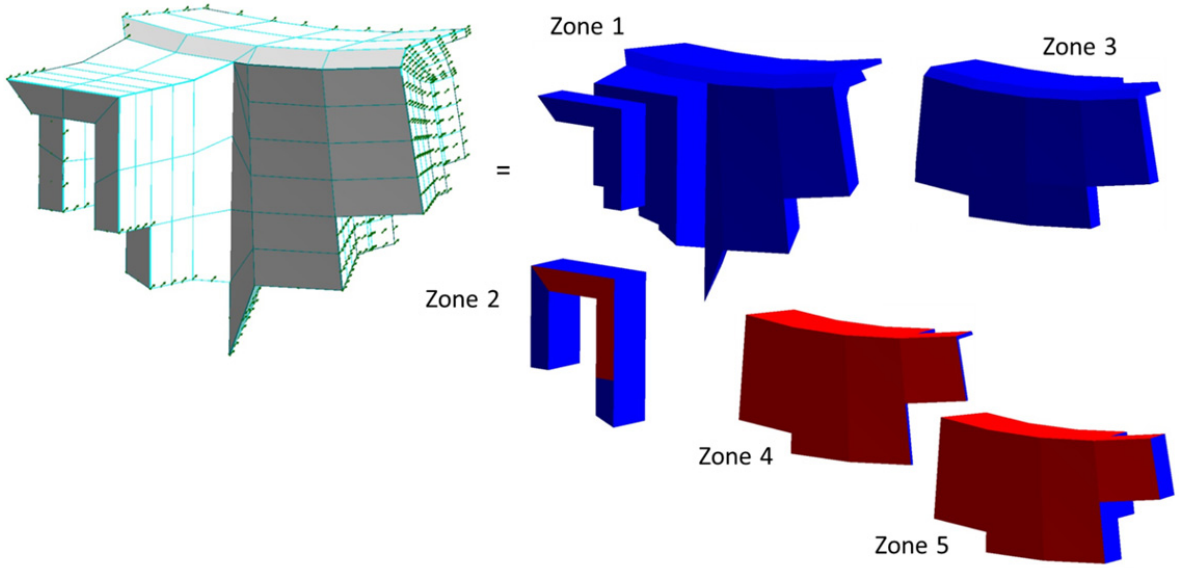

Figure 4: DBEM submodel with highlight of imported displacement boundary conditions on the cutting surfaces and related subdivision in zones.

	Zone 1	Zone 2	Zone 3	Zone 4 (orthotropic)	Zone 5 (orthotropic)
Young Modulus (MPa)	0.158e+06	0.197e+06	0.230e+05	E_x=11600 E_y=25400 E_z=25400 ν_{xz} =ν_{xy}=0.15 ν_{yz}=0.11 G_{xy}=G_{xz}=3070 G_{yz}=3370	E_x=20951 E_y=22281 E_z=38387 ν_{xy}=0.28 ν_{xz} =0.17 ν_{yz}=0.172 G_{xy}=8103 G_{xz}=4314 G_{yz}=8540
Poisson ratio	0.30	0.28	0.32		
Linear expansion coefficient	0.104e-04	0.102e-04	0.121e-04	1.42e-05	1.18e-04

Table 1: Material properties at 4 K temperature.

In Fig. 5 the DBEM submodel is shown, in the configuration before and after the crack insertion (it is possible to see the remeshing in the cracked area); the maximum principal stresses (MPa) in correspondence of the electromagnetic load equal to 3 Tesla (T) and at a temperature equal to 4 K, are calculated with a DBEM thermal-stress analysis [6]; the structural boundary conditions are the displacement on the cutting boundaries as imported from the FEM model; the initial crack is semicircular with a radius equal to 7 mm.

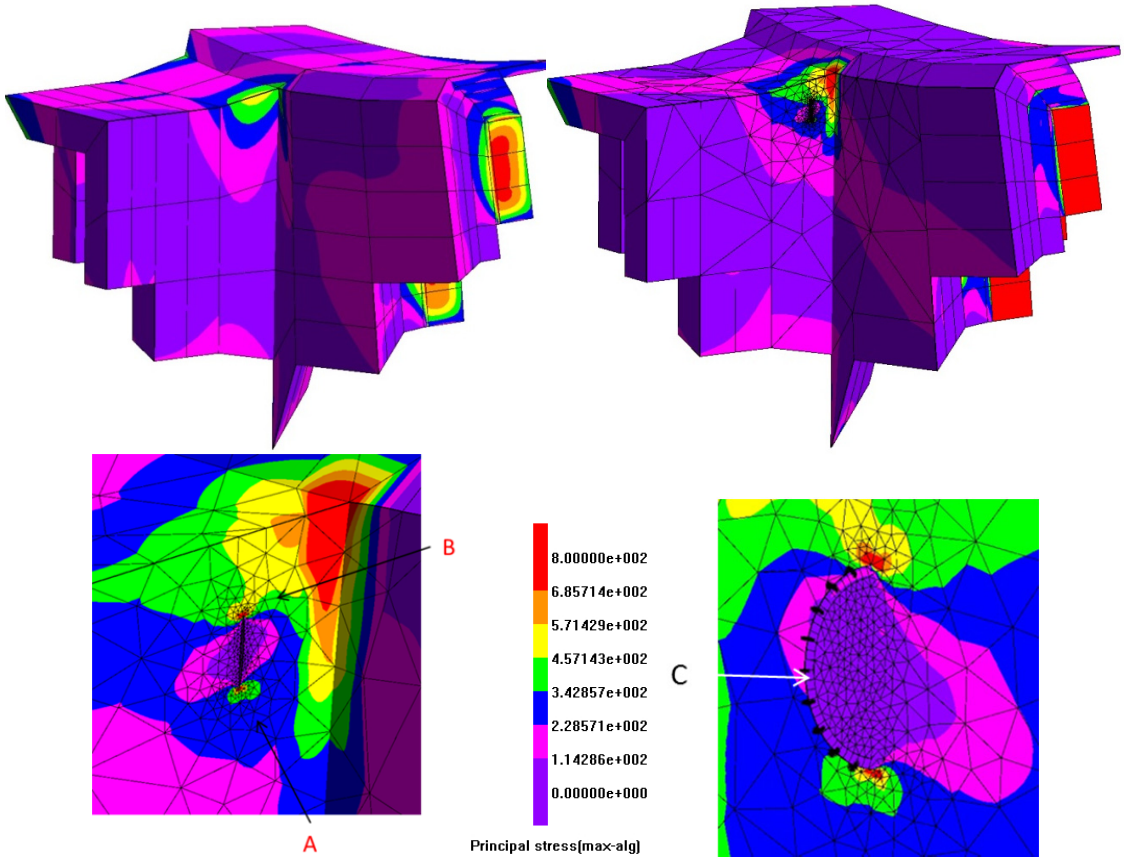

Figure 5: DBEM submodel, before and after crack insertion (with different views), with highlight of Maximum Principal stresses (MPa).

The crack propagation law adopted is the Paris law (Eqn.2) calibrated under cryogenic conditions (T=4K) [2]:

$$\frac{da}{dN} = C\Delta K^m \tag{2}$$

with C=7.95e-13 (with da/dN measured in m/cycle and ΔK in MPa*m$^{0.5}$) and m=3.23. The fatigue cycle considered is based on the coil cooling, from ambient temperature to 4 K, and subsequent application of the electromagnetic load corresponding to a magnetic field cyclically varying from 0 to 3 T.
After 6 steps of crack propagation, the crack front break through the LSE superior surface as shown in Fig. 6, where again the maximum principal stresses (MPa) and the final crack shape are shown.

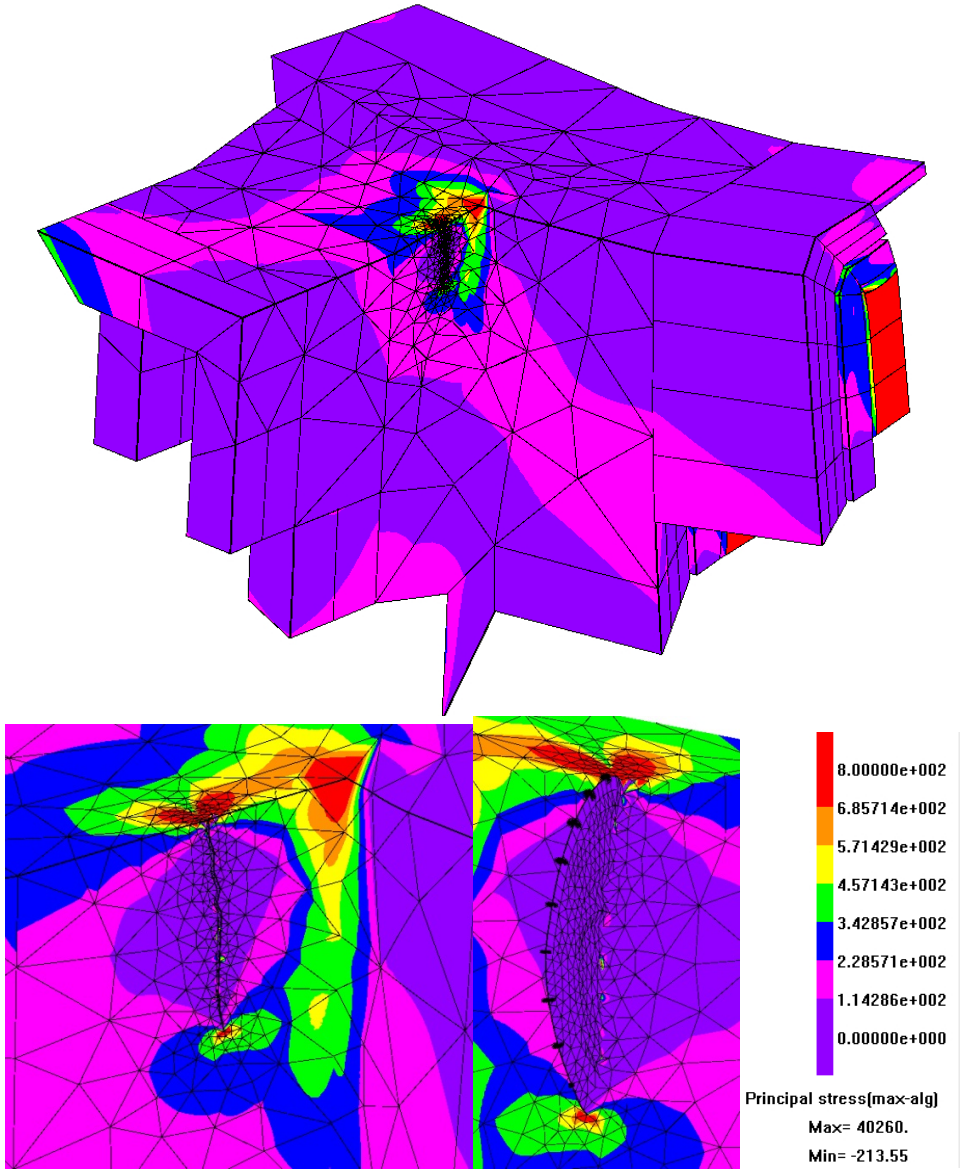

Figure 6: DBEM submodel, in the final cracked configuration (with different views), with highlight of Maximum Principal stresses (MPa).

The mode I SIFs (model II and mode III SIFs are much lower) along the crack front for each step of crack advance are shown in Fig. 7: it is possible to see the sudden increase of KI, in the final step, along that part of the crack front that break through the upper LSE surface (see Fig. 6).

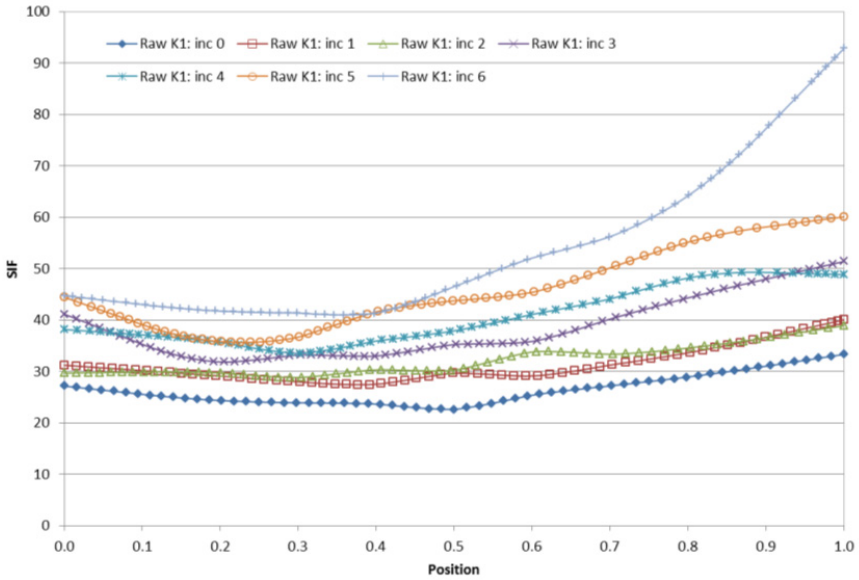

Figure 7: mode I SIFs (MPa*m$^{0.5}$) along the crack front for each step of crack advance.

One of the aims of this work was to check the influence on the fatigue cycles of a different crack front initial shape, so it was also considered an alternative case with an initial semielliptical crack with the same value of a=7 mm and with a depth reduced from c=7 to c=5 mm. The fatigue cycles for each crack advance for the two aforementioned initial configurations are shown in Fig. 8: it is clear the non negligible effect of the initial crack geometry.

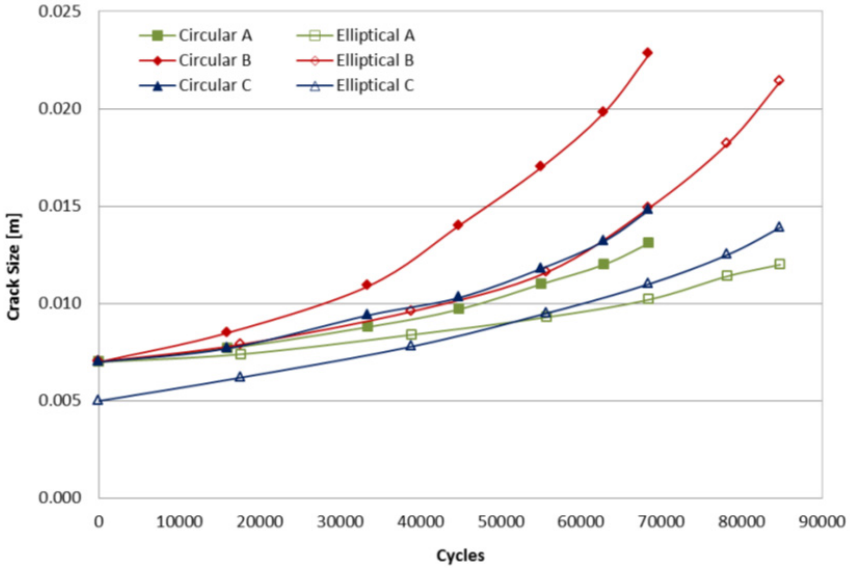

Figure 8: Fatigue cycles vs. semielliptical axis length (m) for an initial semicircular or elliptical crack.

The second aim of this work was to analyse the reciprocal influence of adjacent cracks and consequently a multiple crack propagation analysis has been performed.
The two initial cracks considered are respectively semicircular, with radius equal to 7 mm (the N.1 in fig. 9a), and semielliptical (N. 2 in fig. 9a) with semiaxis a and c (depth size) respectively equal to 7 mm and 5 mm; the distance between the centres of the two aforementioned cracks is equal to 28 mm; the corresponding stress scenario is illustrated in Fig. 9a. The stress scenario and the crack configuration after four steps of crack propagation are shown in Fig. 9b: it is possible to see that from this stage on the crack coalescence can be considered likely to happen.

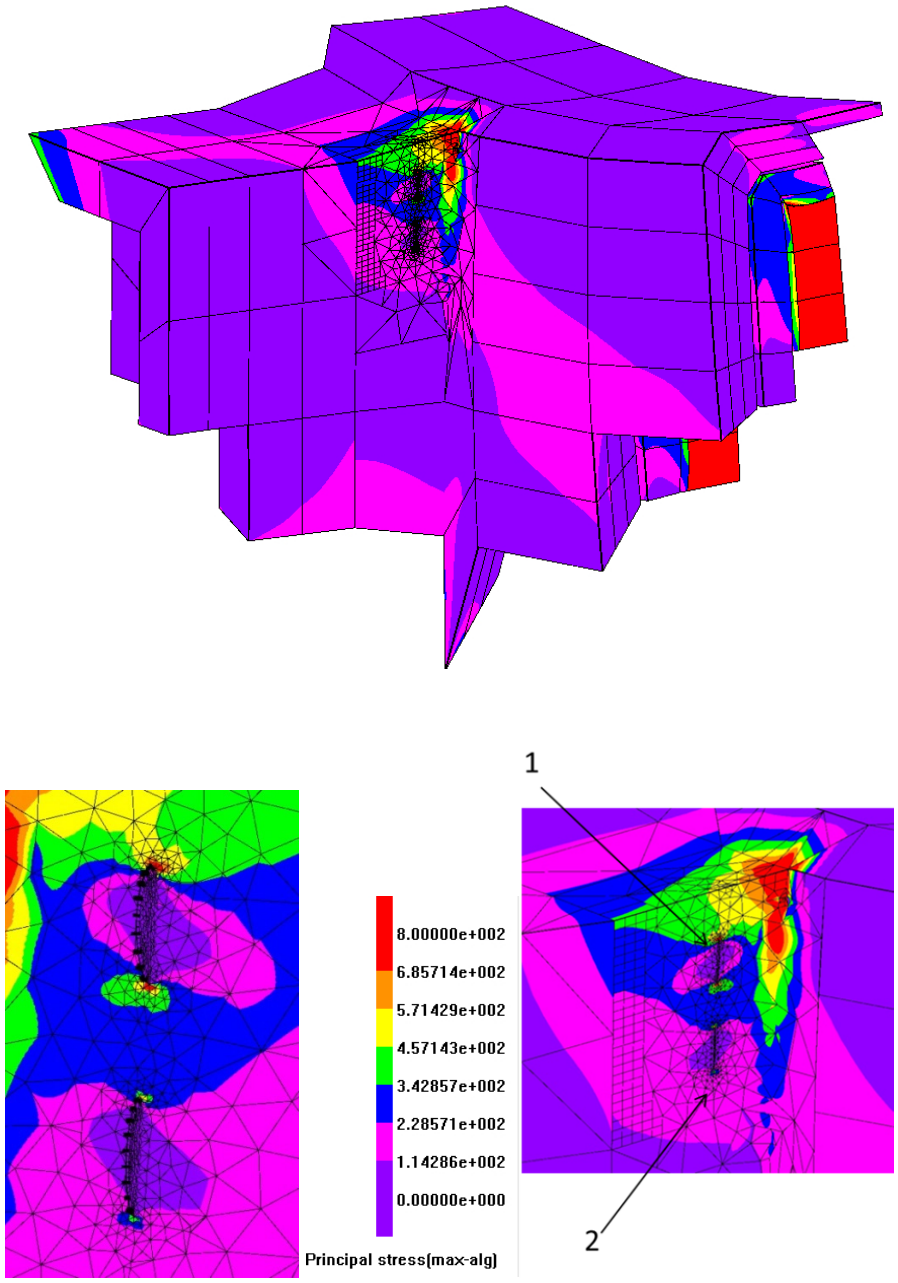

Figure 9a: DBEM submodel, in the initial multiple cracked configuration (with different views), with highlight of Maximum Principal stresses (MPa).

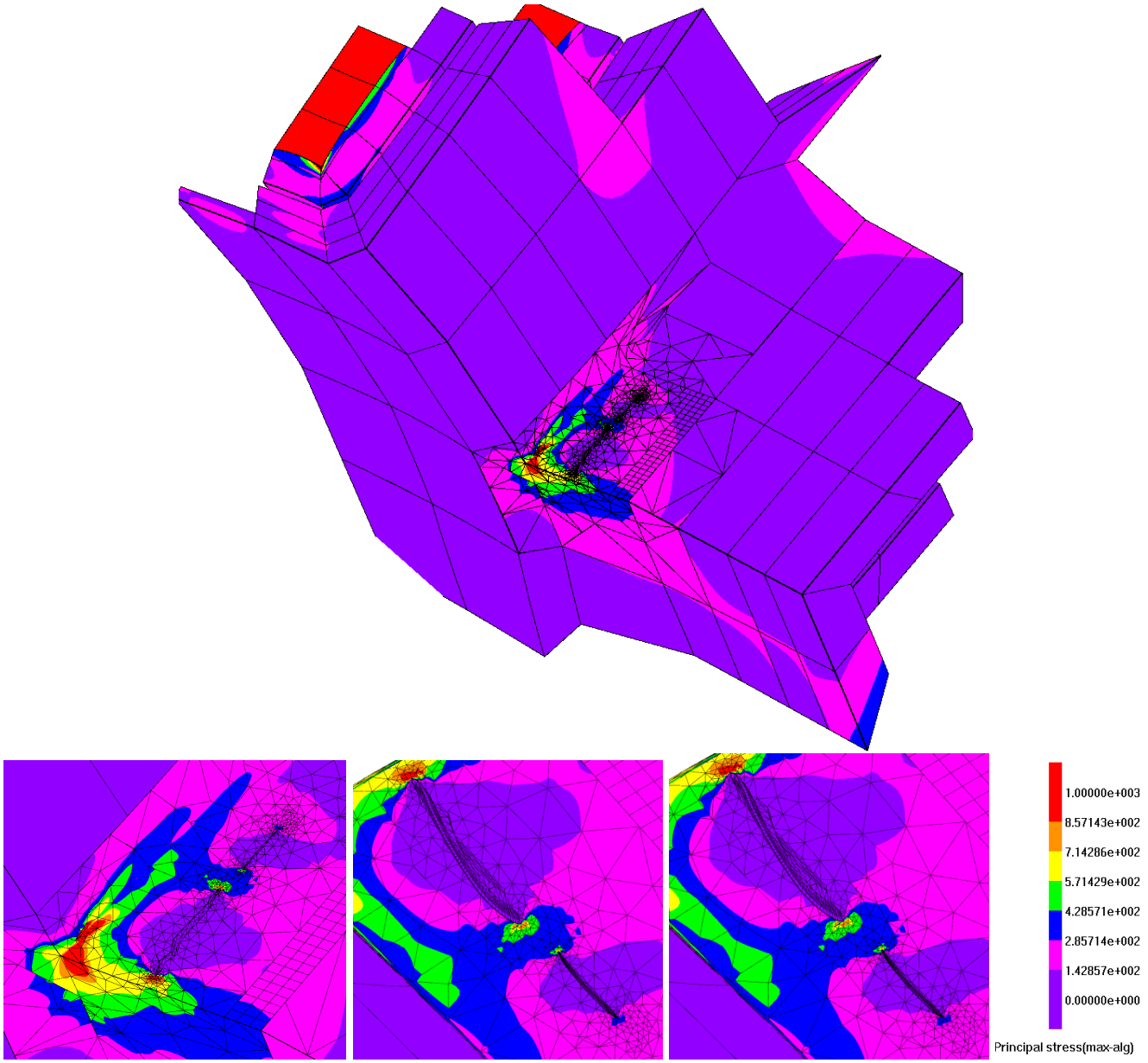

Figure 9b: DBEM submodel, in the final multiple cracked configuration (with different views), with highlight of Maximum Principal stresses (MPa).

Differently for the previous case, this time the SIFs are calculated by the crack opening displacement method (COD) [3] and are shown for the two cracks at each crack advance in Figs. 10-13. With reference to Fig. 13 it is to be pointed out the formula used (Eqn. 3) for calculating the equivalent SIF [7]:

$$K_{eq} = \sqrt{((K_I + |K_{III}|)^2 + 2K_{II}{}^2)} \quad (3)$$

The fatigue cycles for each crack propagation step for the two aforementioned cracks are shown in Fig. 14: comparing the double crack results with the single crack results (Fig. 8) it is possible to observe a clear detrimental effect of the second crack on the main semicircular crack (e.g. in case of multiple cracks, the main crack depth reaches a size of 2 mm after 45000 cycles rather than after 65000 cycles as in the single crack case).

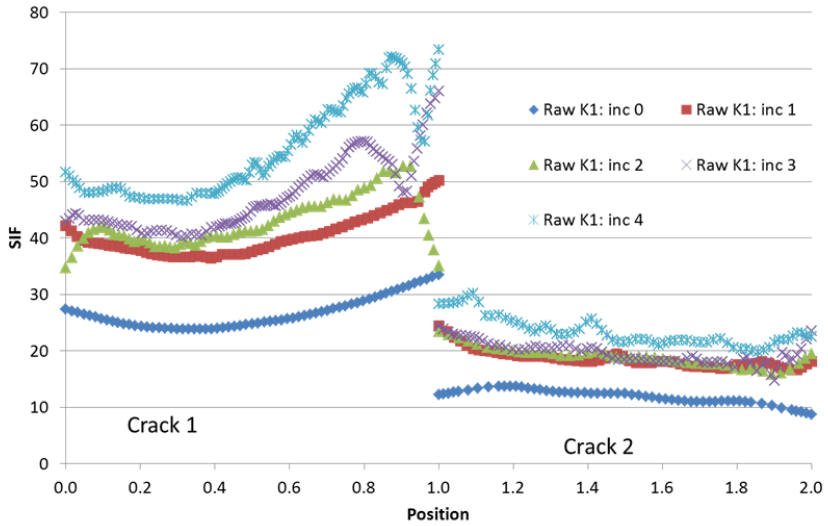

Figure 10: mode I SIFs (MPa*m$^{0.5}$) along the crack front for each step of crack advance for cracks N. 1 and 2.

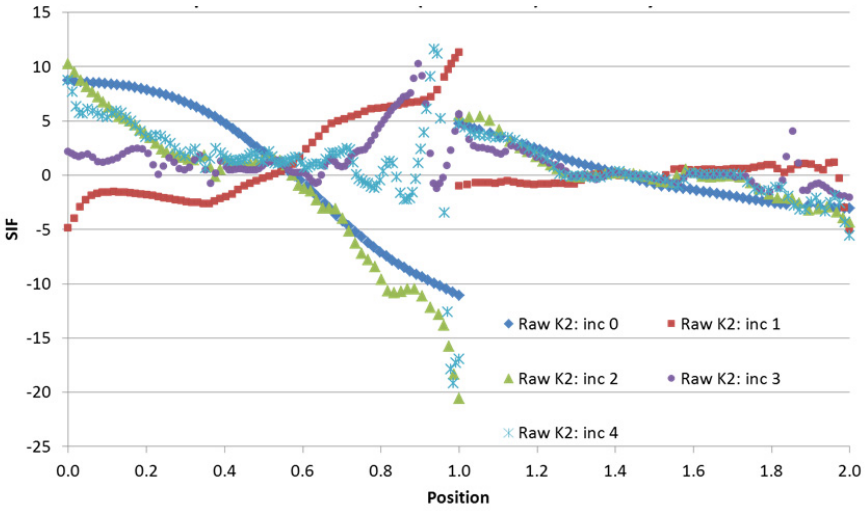

Figure 11: mode II SIFs (MPa*m$^{0.5}$) along the crack front for each step of crack advance for cracks N. 1 and 2.

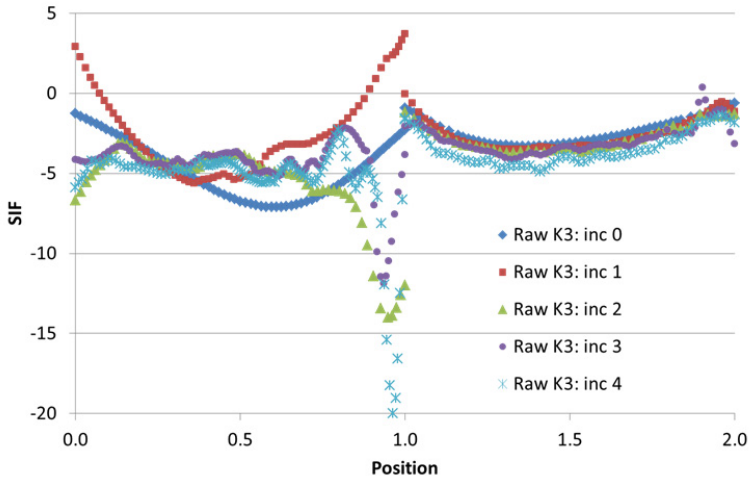

Figure 12: mode III SIFs (MPa*m$^{0.5}$) along the crack front for each step of crack advance for cracks N. 1 and 2.

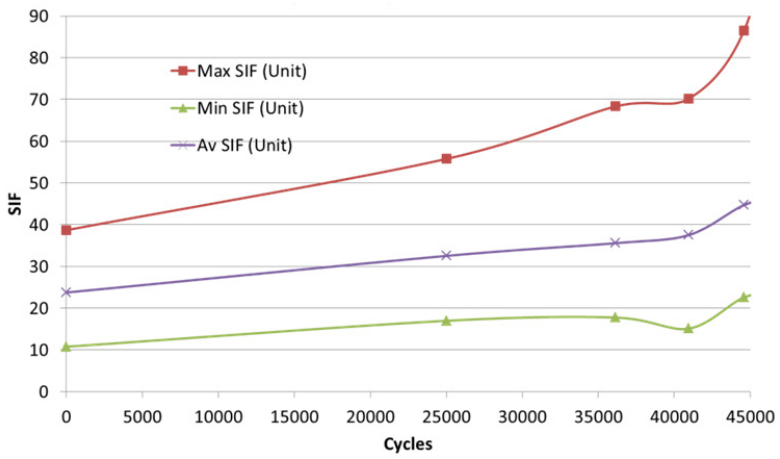

Figure 13: Maximum, minimum and average equivalent SIF (MPa*m$^{0.5}$) for each step of crack advance for cracks N. 1 and 2.

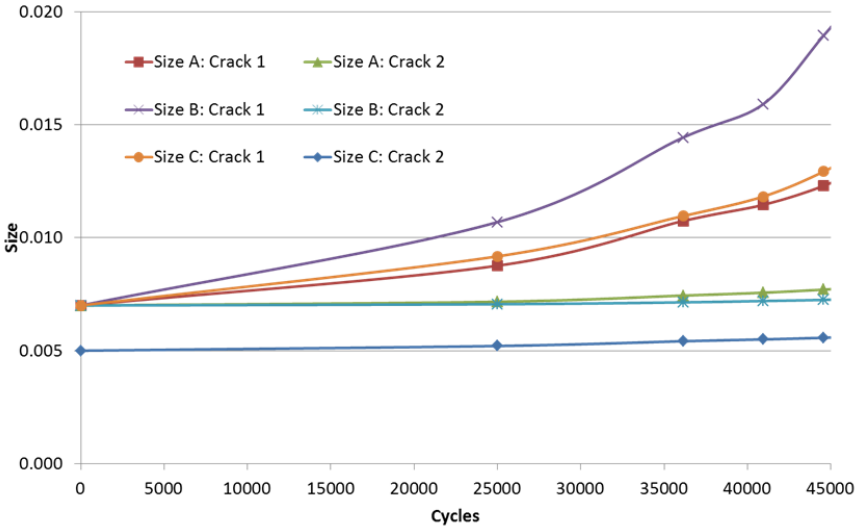

Figure 14: Crack size vs. fatigue cycles.

CONCLUSIONS

In this paper some partial results of a benchmarking activity between two different approaches for the crack growth assessment in a component of the magnet system of Wendelstein 7-X are presented: both approaches are based on the submodelling of the critical cracked domain, as extracted from an FEM overall model, but in one case the submodel is still FEM based whereas in the second case the submodel is DBEM based. The latter approach realises a synergic coupled approach between the two numerical procedures, providing a more flexible tool for analysing complex crack scenarios. The adopted codes are ANSYS and ABAQUS for the FEM modelling and BEASY for the DBEM modelling.

REFERENCES

[1] V. Bykov, F. Schauer, K. Egorov, A. Tereshchenko, P. van Eeten, A. Dübner, M. Sochor, D. Zacharias, A. Dudek,W. Chen, P. Czarkowski, L. Sonnerup, J. Fellinger, D. Hathiramani, M.Y. Ye,W. Dänner, W7-X team, Fusion Engineering and Design, 84 (2009) 215.
[2] J. Fellinger et al.:, Fus. Eng. Des. (2012), http://dx.doi.org/10.1016/j.fusengdes.2012.11.021 (in press)
[3] R. Citarella, G. Cricrì, Engineering Fracture Mechanics, 77 (2010) 1730.

[4] R. Citarella, G. Cricrì, M. Lepore, M. Perrella, In: Advanced Structured Materials with Complex Behaviour, Edited by A. Öchsner, L.F.M. da Silva, H. Altenbach Materials. Springer-Verlag, Berlin, Germany, 3(2) (2010) 181.
[5] R. Citarella, M. Perrella, Fatigue and Fracture of Engineering Material and Structures, 28 (2005) 135.
[6] R. Citarella, M. Lepore, C. Caliani, M. Perrella, In: Proceedings of The 4th International Conference on "Crack Paths" (CP 2012), Gaeta, Italy, (2012).
[7] Y. Mi , Three Dimensional Dual Boundary Element Analysis of Crack Growth, PhD thesis.